Burner-heated dehydrogenation of a liquid organic hydrogen carrier (LOHC) system

Jonas Bollmann[a,b,c],Kerstin Mitländer[f], Dominik Beck[a], Patrick Schühle[f], Florian Bauer[a,b], Lars Zigan[a,b,c,d], Peter Wasserscheid[c,e,f], Stefan Will[a,b,c]

[a] *Lehrstuhl für Technische Thermodynamik (LTT), Friedrich-Alexander-Universität Erlangen-Nürnberg (FAU), Am Weichselgarten 8, D-91058 Erlangen, Germany*

[b] *Erlangen Graduate School in Advanced Optical Technologies (SAOT), Friedrich-Alexander-Universität Erlangen-Nürnberg (FAU), Paul-Gordan-Str. 6, D-91052 Erlangen, Germany*

[c] *Energie Campus Nürnberg, Fürther Str. 250, D-90429 Nürnberg, Germany.*

[d] *present address: Institut für Thermodynamik, Professur für Energiewandlung, Fakultät für Luft- und Raumfahrttechnik, Universität der Bundeswehr München (UniBw M), Werner-Heisenberg-Weg 39, D-85577 Neubiberg, Germany.*

[e] *Forschungszentrum Jülich, Helmholtz-Institute Erlangen-Nürnberg for Renewable Energy (IEK 11), Egerlandstr. 3, D-91058, Erlangen, Germany*

[f] *Lehrstuhl für Chemische Reaktionstechnik (CRT), Friedrich-Alexander-Universität Erlangen-Nürnberg (FAU), Egerlandstr. 3, D-91058, Erlangen, Germany*

Abstract

For a hydrogen-based economy, safe and efficient hydrogen storage is essential. Compared to other chemical hydrogen storage technologies, such as ammonia or methanol, liquid organic hydrogen carrier (LOHC) systems allow for a reversible storage of hydrogen while being easy to handle in a diesel-like manner. In our contribution, we describe for the first time the successful utilization of the exhaust gas enthalpy of a porous media burner to directly supply the dehydrogenation heat for a kW-scale dehydrogenation of the hydrogen-rich LOHC compound perhydro dibenzyltoluene (H18-DBT). Our setup demonstrates the dynamics of the dehydrogenation unit at a realized maximum hydrogen power of 3.9 kW_{th}, based on the lower heating value of the released hydrogen. For the intended applications with fluctuating hydrogen demand, e.g. a hydrogen refuelling station (HRS) or stationary heating in buildings, a dynamic hydrogen supply from LOHC is important. Methane, e.g. from a biogas plant, is utilized in our scenario as a fuel source for the burner. Hydrogen is released within 30 minutes after cold start of the system. The dehydrogenation unit exhibits a power density relative to the reactor volume of about 0.5 kW_{therm} l^{-1} based on the lower heating value of the hydrogen and a catalyst productivity of up to 0.65 g_{H2} g_{Pt}^{-1} min^{-1} for hydrogen release from H18-DBT. An analysis of the by-products and reaction intermediates shows low by-product formation (e.g. maximum 0.6 wt.-% for high boilers and 0.9 wt.- % for low boilers) and uniform distribution of intermediates after the reaction. Thus, a relatively homogeneous temperature distribution and a uniform LOHC flow in the reaction zone can be assumed. Our findings illustrate the dynamics (heating rates of about 10 K min^{-1}) and performance of direct heating of a release unit with a burner and represent a significant step towards LOHC-based hydrogen provisioning systems at technically relevant scales.

Keywords: Hydrogen storage, LOHC, dynamic heat supply, dehydrogenation, porous media burner

1. Introduction

A hydrogen-based economy requires the storage and transportation of large quantities of hydrogen over long periods and distances [1]. Especially in regions that do not have enough capacities to produce so-called green hydrogen (e.g. due to lack of wind, solar or hydro power or high population density), this is of crucial importance to ensure a permanent and secure availability of hydrogen in sufficient amounts [2, 3]. Due to its high gravimetric energy density of 33.3 kWh kg^{-1} and short refueling times, hydrogen, a particularly clean and climate-neutral energy carrier, has great potential in stationary applications with high energy requirements and mobile applications, such as heavy duty or long-distance freight transport [4, 5]. However, storing hydrogen in the gaseous form is expensive since it has a low volumetric energy density (3 Wh l^{-1}) under atmospheric conditions [2, 6]. In recent decades, several technologies have been explored to solve this challenge and to store large quantities of hydrogen over a long period of time and in a dense and safe form to serve as an energy vector comparable to today's fossil fuels [1, 4, 7-13]. Chemical or physical storage of hydrogen is a very attractive option to meet the desired requirements of a hydrogen-based economy [1, 7, 14]. Chemical hydrogen storage technologies can generally be divided into technologies that use gaseous or liquid compounds as hydrogen-lean storage molecules. CO_2- or N_2-based technologies store hydrogen in the form of methanol or ammonia molecules with high gravimetric energy density (approx. 5 – 6 kWh kg^{-1}). The release of pure hydrogen from the latter, however, requires steam reforming and cracking processes combined with gas separation and purification steps. Hydrogen storage technologies such as liquefied and compressed hydrogen or the use of liquid organic hydrogen carrier systems reach lower gravimetric energy densities (approx. 1.5 – 2 kWh kg^{-1}), but enable much easier production of pure hydrogen [8]. In comparison to methanol, the use of LOHC systems does not emit harmful greenhouse gases (e.g. CO_2) at the point of use. Compared to ammonia, LOHC are easier to handle due to their lower toxicity and liquid aggregate state at ambient temperature [8].

1.1. LOHC technology and heat supply during hydrogen release

In recent years, LOHC systems have gained increasing attention for the transport or storage of large amounts of hydrogen at ambient pressure and temperature [5, 12, 15-19]. LOHC systems are composed of organic compounds that can be catalytically hydrogenated and dehydrogenated in repeated reversible cycles [6, 15, 20]. A liquid storage medium for hydrogen enables storage in simple vessels under ambient conditions, transfer with pumps, and use of existing liquid fuel infrastructure. Exothermic hydrogenation and endothermic dehydrogenation of the carrier molecule can either be performed in the same reactor in the application case of energy storage or in different reactors, in the application case of transportation [17, 21, 22]. LOHC technology also allows the required hydrogen output power (conversion unit) or the energy stored in the LOHC system (storage volume) to be adjusted depending on the demand [16].
The LOHC system dibenzyltoluene (H0-DBT)/ perhydro dibenzyltoluene (H18-DBT) has advantageous properties for industrial applications [15, 18, 23, 24] compared to previously discussed systems, such as toluene/methylcyclohexane [25] or N-ethylcarbazole/perhydro–N-ethylcarbazole [8, 26]. The DBT-based LOHC system was selected for our application due to its high hydrogen storage capacity of 6.2 mass %, high thermal stability, well characterized toxicological and eco-toxicological properties, and excellent commercial availability. In addition, the high boiling point of 390°C (H0-DBT) and the high flash point of 200°C results in good intrinsic safety and simplified handling of this LOHC system [15, 27, 28].
The key process step for hydrogen release is the catalytic dehydrogenation of H18-DBT. Regarding the storage capacity of this LOHC system, 56.6 g of releasable hydrogen is stored in 1 l of H18-DBT. This means that 2.05 kWh of energy is stored in 1 kg of H18-DBT [29, 30]. Typically, the dehydrogenation requires a temperature level between 280°C and 320°C, a Pt/Al_2O_3-catalyst, a low pressure level of 0.1 MPa to 0.5 MPa, and energy in the form of heat [6, 30, 31]. The amount of energy required for the strongly endothermic H18-DBT dehydrogenation is 65 kJ per mol of H_2 (at ambient conditions) [27]. Consequently, 27 % of the lower

heating value of the hydrogen stored in H18-DBT is required to provide the heat for the dehydrogenation reaction. Thus, heat provision and heat integration aspects are an important focus in developing effective hydrogen release processes for this LOHC system [16].

Current LOHC systems typically use catalyst pellets placed in tubes as packed beds [32-34]. Various options are described in the literature to achieve optimal system dynamics and power density of the LOHC dehydrogenation unit if the catalyst-filled reaction volumes are heated from the outside [20, 32, 35-39]. For most published LOHC dehydrogenation applications, heat for the endothermic reaction is supplied via a heat transfer fluid [6, 15, 34, 40]. Previous studies have also described the coupling of the dehydrogenation process with various heat sources [41]. Preuster et al. utilized the waste heat of a solid oxide fuel cell [16] and Hampel et al. applied the exhaust gas enthalpy of a hydrogen-fueled micro gas turbine for dehydrogenation experiments [42]. Furthermore, Schumacher et al. demonstrated the use of waste heat from an internal combustion (IC) engine in a simulation study [43]. Krieger et al. presented a theoretical concept and simulations for coupling the LOHC dehydrogenation process with industrial waste heat [44]. Rao et al. [45] simulated the optimization of a LOHC dehydrogenation system by supplying energy with a hydrogen burner. Badakhsh et al. [46] demonstrated LOHC dehydrogenation using a highly integrated heat pipe reformer with a hydrogen burner and Ali et al. [47] used a microchannel reactor for the dehydrogenation of perhydro-dibenzyltoluene. Furthermore, with the so-called hot pressure swing reactor concept, a design for integrating the heat of hydrogenation for dehydrogenation was presented [17, 29, 48]. The dynamic behavior of the dehydrogenation process in combination with a polymer electrolyte membrane (PEM) fuel cell, was studied by Fikrt et al. [40] and Geiling et al. [39]. While Fikrt et al. improved the dynamic behavior of the dehydrogenation process by pressure changes in the free-volume between the dehydrogenation unit and the PEM fuel cell, Geiling et al. used pressure changes inside the dehydrogenation unit to enable dynamic combined operation of PEM fuel cell and LOHC dehydrogenation unit [39, 40]. Moreover, Müller et al. investigated the potential to combine different types of fuel cells with an LOHC release unit [49] and Haupt et al. used simulations to demonstrate the potential of heat integration via a combined heat and power system [50]. There is still significant potential to increase H18-DBT dehydrogenation performance, especially reactor heating dynamics and efficiency through optimized thermal management. One promising option to achieve this target is the use of a burner for direct heating of the dehydrogenation reactor.

For the specific requirements of this application, i.e. heat dissipation over a broad area and a large power modulation range, a porous media burner seems particularly beneficial. Compared to a burner concept using a free laminar flame [46], such a burner is characterized by increased heat and mass transfer in the reaction zone. The reason for this behavior is the significantly higher conductivity and emissivity of solids compared to gases. A fundamental factor for the penetration of the flame front into the porous medium is the relation between the heat generated by the combustion reaction and the heat dissipation, which results from the heat transport in the reaction zone [51]. The advantages associated with this type of burner include low pollutant formation and high fuel flexibility. A porous media burner can be operated with liquid and gaseous fuels over a wide range of equivalence ratios. The homogeneous temperature distribution on the burner surface of the porous media burner results in low NO_x and CO emissions [51-54]. Furthermore, the variable burner shape and simple burner design were reasons for choosing a porous media burner for this study [51]. Consequently, direct heating of a dehydrogenation unit with a porous media burner via the exhaust gas is a promising approach to achieve dynamic and energy-efficient release behavior.

To the best of our knowledge, no direct heating of a LOHC release unit on a kW-scale using a porous media burner (PMB) has been realized so far. In a previous work of some of us, a small-scale dehydrogenation setup with a maximum hydrogen release of 72 W, heated by a porous media burner was developed [55]. As we have learned from our previous work, this solution offers the advantage of a very dynamic controllability of the heating process in combination with a high heating temperature. The burner exhaust gas volume flow and temperature can be adapted to the requirements of the dehydrogenation plant within a few seconds, simply by adjusting the burner load. In this article, a release unit directly heated by a porous media burner is investigated

at a technically relevant kW-scale, with the reactor developed and designed on the basis of the findings of our previous work.

1.2. Reaction intermediates and by-product formation during the dehydrogenation of H18-DBT

An important factor to be considered in the dehydrogenation of H18-DBT is the formation of reaction intermediates and by-products. In this context, the reaction intermediates are species with partially hydrogenated rings and regioisomers. Thus, up to six DBT species can be formed by dehydrogenation of H18-DBT, each of them consisting of several regioisomers [31]. The by-products formed by undesired side-reactions, can be divided into low boiling components (e.g. toluene, cyclohexane) and higher boiling components (e.g. fluorene derivatives with boiling points >390°C at ambient pressure) [29]. While the traces of low boiling by-products formed during dehydrogenation, such as methane, benzene, toluene, cyclohexane, methylcyclohexane, ethane, carbon dioxide, and carbon monoxide, can be almost completely removed by degassing the LOHC material, some of the high boiling by-products are more difficult to separate without LOHC losses [17, 39, 56]. These high boilers typically represent LOHC substances themselves (they are hydrogenated and dehydrogenated together with the Hx-DBT compounds), but their formation should be limited to a certain amount as they change the physico-chemical properties of the carrier liquid [56]. The content of intermediates and by-products in the reaction product depends on the catalyst [29, 33, 57, 58], but is also influenced by reaction conditions [31]. In particular, the concentration of reaction intermediates can give information about temperature and flow distributions in the reaction volume. As an example, one can assume inhomogeneous temperature and flow distribution if mainly completely unloaded and loaded DBT are present in the product stream. Due to the dynamics of the dehydrogenation reaction, an equal distribution of the reaction intermediates indicates a homogeneous temperature and flow distribution [29, 31, 56]. By monitoring the reaction intermediates and by-products through samples taken in the product stream, we aim to obtain an indication of the temperature and flow distribution in our dehydrogenation unit during the hydrogen release reaction from H18-DBT.

1.3. Aim of this work

The purpose of this work is to demonstrate the feasibility and the advantages of a LOHC dehydrogenation system on a kW-scale heated directly by a porous media burner. In such a setup we aim to investigate the factors influencing hydrogen output and system dynamics during hydrogen release from H18-DBT. A particular focus is on the design and dimensioning of the release unit on a kW scale. The targeted power range defines the required size of the reaction volume, the associated heat transfer area for direct heating with the burner, and the respective burner exhaust gas velocities. In this work, a new design is shown which takes these aspects into account. Our investigation focuses on optimizing power density, overall system efficiency, and heat input to the dehydrogenation unit. In this context, the temperature levels and temperature distributions are investigated via thermocouples. In our case of a technically relevant dimensioned dehydrogenation unit, a further focus is on by-product formation. By-product formation has a significant influence on the required hydrogen purification processes. Moreover, it can be used to identify possible temperature non-uniformities. Therefore, product samples are analyzed for reaction intermediates and by-products.
In this work, a kW-scale hydrogen delivery system for a prototype hydrogen refueling station (HRS) is developed. Since a permanent and safe storage of hydrogen at the refueling station is required, LOHC technology will be used to deliver elemental hydrogen for mobile applications [12, 22]. Compared to existing solutions, we focus on a geometrically adjusted dehydrogenation unit with 4 kW_{th} output power (based on the lower heating value of hydrogen) which is characterized by optimization of heat transfer for direct heating with a porous media burner. The burner is operated with the fuel methane, which may be produced as biomethane using renewable sources resulting in a significant reduction of absolute emissions compared to the use of natural

gas [59]. In this contribution, hydrogen release rates, burner exhaust gas, LOHC temperature levels, and the degree of hydrogenation for various reaction conditions (LOHC mass flows ranging from 1.6 kg h^{-1} to 4.2 kg h^{-1}, average temperature in the reaction volume between 285°C and 320°C and an absolute pressure level between 1.6 bar and 3.3 bar) are presented. Catalyst productivity and hydrogen yield are calculated and compared to values of alternative reactor and heating concepts from the literature. Furthermore, pollutant emissions of the burner are measured during cold start and operation, and contents of reaction intermediates and by-products are analyzed. Finally, the efficiency of the system is determined for specific measurement points.

2. Experimental

2.1. Burner and dehydrogenation setup

The investigation on a directly burner-heated dehydrogenation unit was performed in a self-designed and self-constructed kW-scale setup (see Fig.1), which is located at the Energie Campus Nürnberg.

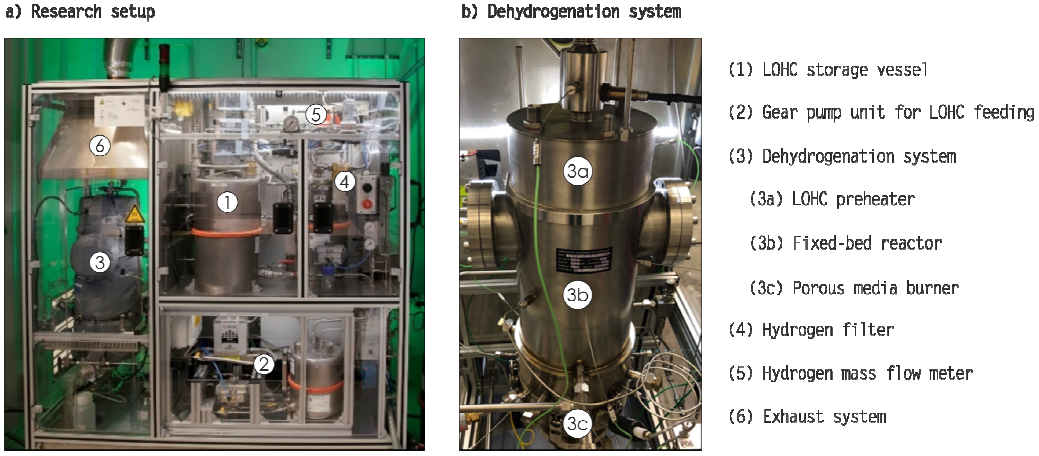

Figure 1: Photograph of a) the research setup for H18-DBT dehydrogenation at the Energie Campus Nürnberg (picture: EnCN / Kristin Zeug) and b) the applied dehydrogenation system in detail with the main components labelled.

The hydrogen release experiments were performed in an in-house built 7.3 l stainless-steel fixed-bed reactor with custom-made thermal insulation (BRA-FLEX, Brandenburger Isoliertechnik GmbH&Co. KG, Germany) and heated by an efficient porous media burner. The burner, specifically developed for our application was operated with the fuel methane (grade 2.5 corresponding to a purity of > 99.5 %, Linde AG, Germany) using a maximum thermal load of 3.0 kW. The methane used can also be produced as biomethane to significantly reduce emissions. Two Bronkhorst mass flow controllers (Bronkhorst High-Tech B.V., Netherlands) controlled the amount of methane and air fed into the burner. For the air volume flow, a F-202AC-RGB (flow range 5 - 150 l_N min^{-1}) and for the methane volume flow, a F-201CV-10K (flow range 0.08 – 15 l_N min^{-1}) flow controllers were used. The equivalence ratio was evaluated using a lambda sensor (type LSU 4.9, Bosch, Germany) positioned in the exhaust gas downstream of the LOHC preheater. The H18-DBT was pumped from the LOHC storage vessel (capacity of about 25 l) via the LOHC preheater into the dehydrogenation unit using a micro annular gear pump (MZR-7245, HNP Mikrosysteme GmbH, Germany). This involved controlling the LOHC mass flow rate with the Bronkhorst Coriolis mass flow meter M15-PGD (flow range 0.2 – 5.0 kg h^{-1}). The volume flow of the released hydrogen was measured using the Bronkhorst mass flow meter F-112AC (flow range up to 60 l_N min^{-1}). The released hydrogen was fed to the exhaust system after flow measurement.

The dehydrogenation experiments were conducted using hydrogenated dibenzyltoluene (H18-DBT, hydrogenation grade > 99 %) purchased from Eastman Chemical Company, United States. For all experiments, the catalyst in the dehydrogenation unit was a 0.3 mass % Pt on alumina eggshell material provided by Clariant Produkte (Deutschland) GmbH. The diameter of the used catalyst spheres was 2 – 4 mm.
Figure 2 shows a schematic flow diagram of the experimental setup. During the dehydrogenation experiments, the gear pump delivers the required amount of H18-DBT controlled by the Coriolis mass flow meter from the storage tank into the fixed bed reactor via the LOHC preheater. A shell and coiled tube heat exchanger with a tube length of 1.3 m, through which H18-DBT flows and which is surrounded by the burner exhaust gas, served as a LOHC preheater. At the point with the highest temperatures calculated in the simulation and measured in preliminary tests, a type K thermocouple is placed to control the maximum temperature inside the dehydrogenation unit. The average temperature in the dehydrogenation unit, which at the same time reflects the set reaction temperature, is determined from the average value of the thermocouples TI 06 to TI 10 (for detailed positions see Figure 4 b), since these are positioned in the area of the release unit close to the burner and thus reflect the highest temperatures achieved in the dehydrogenation unit. During the hydrogen release reaction, a certain amount of evaporated LOHC left the reactor together with the released hydrogen and the liquid LOHC.

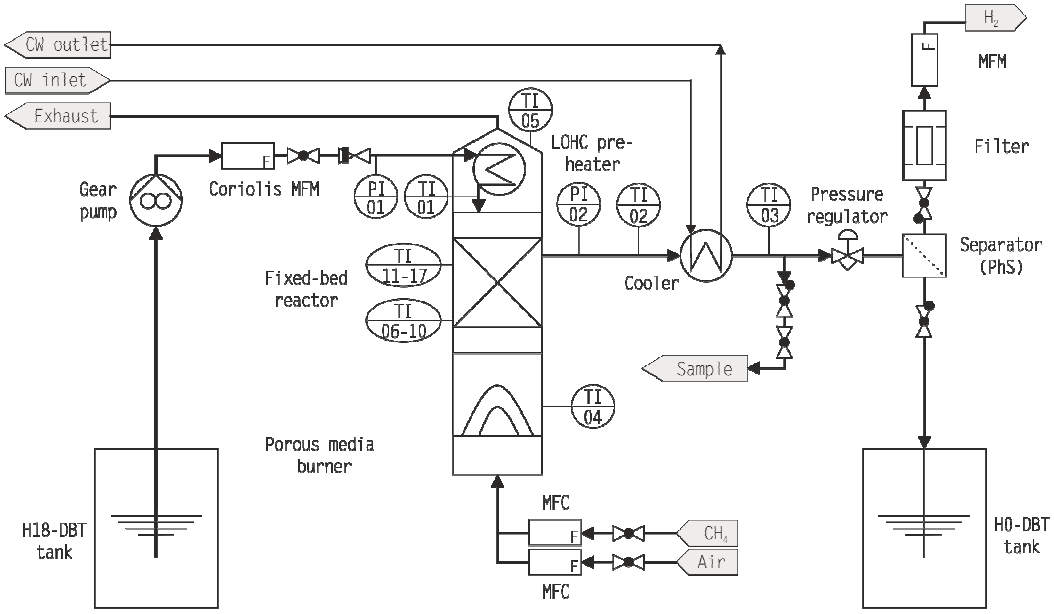

Figure 2: Flow scheme of the experimental setup applied in this work.

A shell and tube heat exchanger served as a partial condenser and cooler after the dehydrogenation unit. After the cooler, a liquid sample can be taken for each measurement point via an integrated mechanism. The H_2, the liquid LOHC, and evaporated components were subsequently split up in a tank that was used as phase separator. Downstream the separator, the volumetric flow rate of the released hydrogen was recorded after passing a porous filter (porosity: 30 µm) using the MFM described above and the unloaded LOHC was stored in the H0-DBT tank. All flowmeters had been calibrated and ensured high dosing accuracy in the required measuring range.
Several type K thermocouples (TI01 – TI03 and TI05 – TI17) with a diameter of 1.5 mm (tolerance class 1) were used for temperature measurements. Due to the high temperature load in the combustion chamber, a type S thermocouple (TI 04) with a diameter of 1.5 mm (tolerance class 2) equipped with a protective ceramic tube

was used for exhaust gas temperature measurements, halfway between the burner and the dehydrogenation unit. All thermocouples (TC Mess- und Regeltechnik GmbH, Germany) used were calibrated. The pressure in the dehydrogenation unit was set by a back-pressure regulator (HF Series, Equilibar, United States) and monitored by two pressure transmitters (SML Series, ADZ Nagano GmbH, Germany). The entire research setup was automatically controlled by a programmable logic controller (X20 system, B&R Automation, Austria) to obtain reproducible experimental results.

2.2. Dehydrogenation system

The in-house built dehydrogenation system consisted of a LOHC preheater and a hydrogen release unit, which in combination with a porous media burner was designed to achieve a kW-scale hydrogen production rate. The shape of the release unit was adapted to the requirements of efficient heat transfer from the burner exhaust gas to the heating of the hydrogen release reaction. A 3-D model of the system is displayed in Figure 3. The objective of our system is an efficient and dynamic hydrogen release from H18-DBT. This requires the heat to be transferred as uniformly as possible into the reaction volume in order to drive the endothermic dehydrogenation reaction.

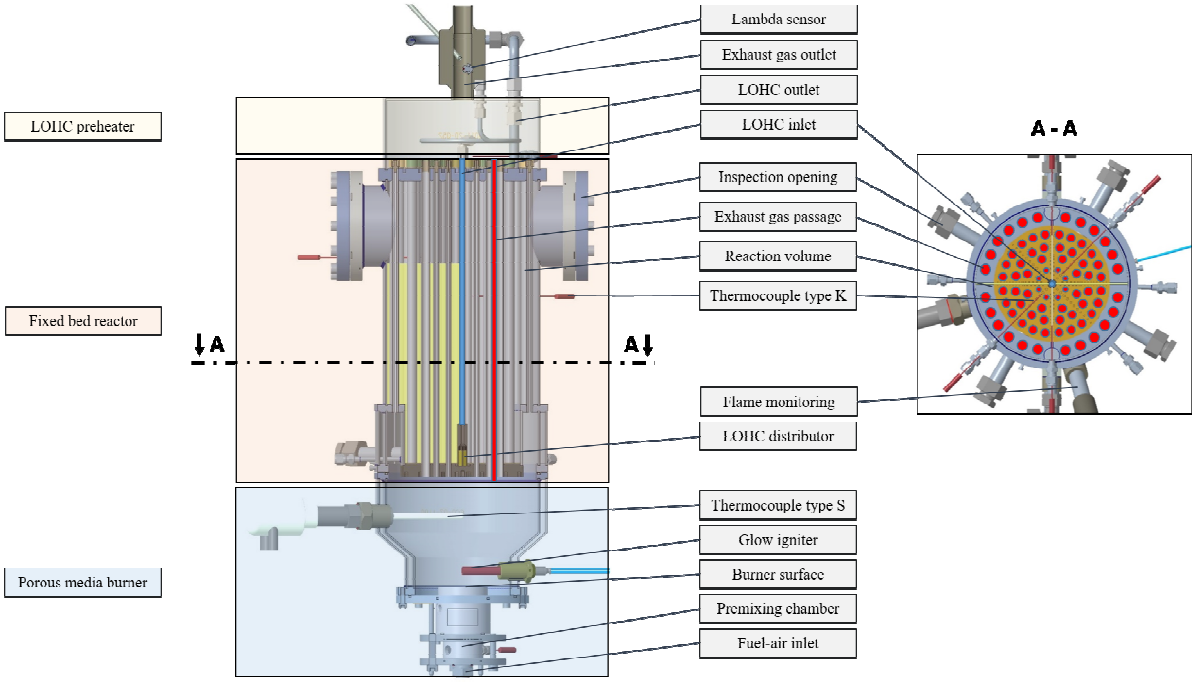

Figure 3: Design of the dehydrogenation system consisting of a LOHC preheater, a fixed bed reactor and a porous media burner as applied in the experiments of this study.

To achieve the aforementioned goals, a system similar to a shell-and-tube heat exchanger was designed with a cylindrical reaction volume, traversed by a large number of tubes of different diameters in which the burner exhaust gas flows. In this way, a large reaction volume is achieved while reducing the overall dimensions of the reactor. This arrangement is in contrast to most of the existing dehydrogenation reactors published in the literature, where the reaction takes place in the tubes and the heating medium flows around them [32, 34, 36]. The reaction volume is evenly traversed by tubes in order to achieve a uniform heat input. The number of tubes

(80 pieces) is defined by the size of the catalyst pellets (approx. 2 - 4 mm in diameter) and by a small distance (approx. 8 mm) between the outer surfaces of the individual tubes. The diameter of the individual tubes was determined from the required guidance of the exhaust gas flow. Since the burner surface is small in relation to the cross-sectional area of the dehydrogenation unit, the exhaust gas flow must be broadened. The guidance of the exhaust gas flow should thereby be controlled via the flow resistance of the individual exhaust gas tubes. Since the diameter of a tube generally has a major influence on the resulting flow resistance, this effect can be used to control the flow distribution of the exhaust gas. This is realized by means of small diameters of the tubes through which the exhaust gas flows above the burner surface, resulting in greater flow resistance, and a larger diameter of the outer exhaust gas tubes, which are not placed above the burner surface. As a result, a uniform distribution of the exhaust gas flow in the dehydrogenation volume is achieved. Suitable tube diameters were selected on the basis of existing stock diameters and with the aid of a flow simulation using STAR-CCM+ software (Siemens PLM Software, Germany).

The overall system has an outer diameter of 235 mm and a length of about 900 mm. For our experiments, the system is arranged vertically, with the burner at the bottom, followed by a combustion chamber, the fixed bed reactor, and the LOHC preheater on top. The fixed bed reactor is heated by the porous media burner, using convective heat transfer through the exhaust gas and radiative heat through the burner surface.

The burner is ignited by a glow igniter located above the burner surface. The flame in the porous medium is analyzed by an optical system for flame monitoring via an optical access in the combustion chamber. The burner itself consists of the premixing chamber and the combustion zone and is made from stainless steel. In the premixing chamber, biomethane and air are mixed according to the desired equivalence ratio. A perforated plate separates the mixing zone from the combustion zone, which is filled with a flame trap made of aluminum oxide and a SiSiC (silicon infiltrated silicon carbide) foam in which combustion takes place. A detailed description of a similar burner can be found in [55]. To characterize the exhaust gas flow and the equivalence ratio, a lambda sensor and a sampling spot were located at the exhaust gas outlet after the LOHC preheater. Emission measurements were performed using an exhaust gas measuring device (Testo 350XL, Testo SE & Co. KGaA, Germany).

The size of the reaction volume is iteratively determined by, on the one hand, the desired hydrogen production rate and, on the other hand, by the heat transfer area required for the energy input. In a first step, the required reaction volume is estimated based on the desired hydrogen production rate of, in our case, about 4 kW_{th} based on the lower heating value of hydrogen. From this specification, the required hydrogen volume flow rate at reaction temperature results. Using catalyst productivities for comparable reactors from the literature [29, 30, 38, 60], the required catalyst mass can be determined first, followed by the catalyst volume using the associated densities of the support structure and the active material. The Hx-DBT input volume flow at reaction temperature in turn results from the expected fraction of hydrogen released per pass through the reaction volume, which depends on the residence time of the Hx-DBT in the dehydrogenation unit. Literature values provide a good indication of the proportion of stored hydrogen released as a function of the residence time for specific reaction parameters (e.g. temperature and pressure) [32, 33, 61]. Based on the Hx-DBT input volume flow rate derived using the above method, the Hx-DBT and the hydrogen volume in the reaction volume at reaction conditions are obtained. Then, the reaction volume required for the desired hydrogen production rate can be determined iteratively by the catalyst volume and by adjusting the required residence time (this leads to the variable Hx-DBT volume and hydrogen volume mentioned above).

In the second step, the required heat transfer area and thus the final reaction volume is determined as follows. Based on the maximum required temperature in the reaction volume of 320°C, the amount of energy to be introduced for the H0-DBT / H18-DBT system of 65 kJ mol^{-1} H_2 [27] for the desired hydrogen production rate of 4 kW_{th} and the exhaust gas temperatures of the porous media burner used determined in preliminary tests, the resulting average temperature can be calculated. Underlying the aforementioned geometric specifications for the fixed bed reactor, the determined preliminary reaction volume and the temperature-dependent LOHC and exhaust gas volume flows resulting from the first mentioned calculations, the minimum required length of

the fixed bed reactor can be calculated. Finally, the resulting geometric dimensions are iteratively adjusted until all the mentioned reaction volume requirements are met. According to the results of the analyses, the reaction volume was filled with 1000 g of the Pt on alumina catalyst.
Figure 4 shows a detailed illustration of the fixed bed reactor on the left and the positions of the thermocouples inside the dehydrogenation reactor on the right. Approximately half of the dehydrogenation volume between the exhaust gas passages (red circles in the Figure 4) is filled with the catalyst. In our experiments, the hydrogenated H18-DBT entered the reactor from the top coming from the preheater and flew through a 4 mm inner diameter tube along the entire length of the reaction volume to the LOHC distributor at the bottom. In this way, the H18-DBT is at reaction temperature when entering the catalyst bed downstream of the distributor. The LOHC distributor provides an inflow of H18-DBT into the fixed bed reactor that is uniformly distributed over the reaction volume (see white arrows in Figure 4 a). The reaction volume has an approximately cylindrical shape with a diameter of about 200 mm and a length of about 360 mm. The inlet has an inner diameter of 4 mm and there are two outlets, each with an inner diameter of 10 mm. The inlet and the two outlets are located at the top of the reaction volume.

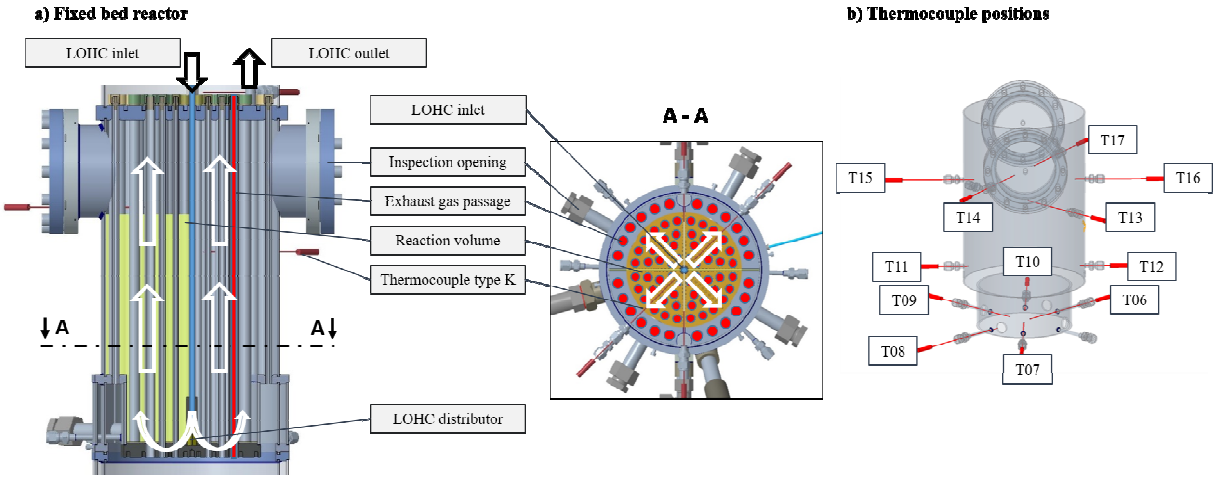

Figure 4: Internal design of the applied dehydrogenation unit (a) and positions of the thermocouples inside the fixed bed reactor (b).

There are twelve K – type thermocouples located at different positions inside the reaction volume (numbers 06 to 17 in Figure 4b). Thermocouples numbered 06 to 10 are located in the catalyst bed at the bottom of the dehydrogenation volume at various distances from the central axis. Thermocouples numbered 11 and 12 are placed approximately halfway downstream the catalyst bed at the outer boundary of the reaction volume. The thermocouples numbered 13 to 17 are located in the upper part of the reaction volume. These are also installed at different distances from the central axis. The location and distribution of the thermocouples in the dehydrogenation unit were determined using the results of heat-up experiments and simulations with STAR-CCM+ software (Siemens PLM Software, Germany). In this way, the temperature distribution within the reaction volume can be estimated and the approximate starting point of the reaction can be determined. Thermocouple number 09 is used to set and maintain the reference temperature via the programmable logic controller (PLC), since the highest temperature was measured there in preliminary heat-up experiments. Since there is a temperature spread in the reactor, the highest temperature is reached at the bottom of the dehydrogenation unit, and a significant part of the reaction rate occurs at the bottom, the average temperature ϑ_{mD} is formed from the temperature readings of the thermocouples numbers 06, 07, 08, 09 and 10. The present

value of the pressure is monitored by two pressure transmitters. There are two inspection openings on the top of the fixed-bed reactor for cleaning and inspection purposes.

2.3. Hydrogen release experiments

In this study, the described dehydrogenation system with a porous media burner is investigated with regard to its heating and dehydrogenation efficiency. Therefore, parameters like the temperature and pressure in the fixed bed reactor, the H18-DBT mass flow, and the power of the biomethane burner are varied. The temperatures of the exhaust gas before and after the reactor, the temperatures at the various thermocouple locations, the pressure in the dehydrogenation unit, the time until hydrogen release starts in the system, the hydrogen volume flow and the LOHC mass flow are measured. To determine the degree of hydrogenation (DoH) and the rate of by-product formation, samples are taken during the reaction. Furthermore, the dehydrogenation efficiency is evaluated by calculation of the hydrogen mass flow. Hydrogen yields, catalyst productivities and hydrogen production rates are also determined. In addition, pollutant emissions of the methane-fueled porous media burner are measured during cold start and stable operation.
At the beginning of each measurement day, the system is heated for 90 minutes starting with an initial temperature of about 23 °C. Measurements are conducted using different reaction conditions (e.g. pressure, temperature and mass flow of H18-DBT in the fixed bed reactor). The H18-DBT mass flow is adjusted with the Coriolis mass flow meter and is preheated on the way into the fixed bed reactor. The burner is operated at a power range of 0.6 kW to 3.0 kW and an equivalence ratio of 0.83 throughout all measurements. This equivalence ratio is chosen because it allows for stable and reliable operation of the porous media burner in the required power range. The burner is operated dynamically and is controlled by a proportional-integral-derivative (PID) controller to automatically attain and maintain the set temperature.
In advance, preliminary tests and a performed Pareto analysis were used to define the measurement points, shown in Table 1. The temperature parameter from Table 1 represents the average temperature ϑ_{mD} described in section 2.2.

Table 1:Overview of the experiments.

	Parameters		
Experiment	Average temperature ϑ_{mD} / °C	Mass flow rate LOHC / kg h^{-1}	Pressure / bar (absolute)
exp.1	280	1.6	2.0
exp.2	280	2.9	2.0
exp.3	280	4.2	2.0
exp.4	300	1.6	2.0
exp.5	300	2.9	2.0
exp.6	300	4.2	2.0
exp.7	320	1.6	2.0
exp.8	320	2.9	2.0
exp.9	320	4.2	2.0

Initially, only the temperature and the LOHC mass flow in the fixed bed reactor are varied, since pressure influence on the release reaction is shown to be small in the preliminary experiments. Therefore, a pressure variation is only carried out for a selected measurement point. Each measurement point is maintained for 90 minutes, with the first 30 minutes serving to stabilize the system. In this way, the system runs for about 60 minutes for each measurement point once constant boundary conditions are achieved. The generated measurement data are stored in time intervals of 1 s. During one measurement day, four to five measurement points can be investigated. The last measurement point of a day is a repetition of a previous measurement point

to ensure reproducibility of the results. At the end of each measurement point, a LOHC sample of approximately 20 ml is taken for further analysis.
To investigate repeatability, the measurements displayed in the next section have been performed at least two times. The data shown represents the average of these at minimum two measurements, unless otherwise noted. The resulting temperatures in the fixed bed reactor and the exhaust system are recorded with a measurement accuracy of 5 K (manufacturer information). Two pressure transmitters with a 0.01 bar measurement accuracy are used to track the pressure within the dehydrogenation unit. During the measurement time interval, the pressure fluctuations in the reactor were less than ± 0.5 %. The fluctuation of the mean temperature in the reaction volume between the individual runs was less than ± 5.0 %, while the fluctuation of the hydrogen volume flow was about ± 3.0 %.
The calculations for the quantitative evaluation of the dehydrogenation reaction are as follows. The hydrogen production rate $\dot{H}_{H_2}(t)$ (W) after time t (s) is calculated based on the hydrogen mass flow $\dot{m}_{H_2}(t)$ (kg s^{-1}) and the lower heating value of hydrogen LHV_{H_2} (120.0 MJ kg^{-1}):

$$\dot{H}_{H_2}(t) = LHV_{H_2} \cdot \dot{m}_{H_2}(t). \quad (1)$$

The hydrogen mass flow rate (kg s^{-1}) is determined using the measured hydrogen volume flow $\dot{V}_{H_2}(T)$ (l_N s^{-1}) and the corresponding hydrogen density $\rho_{H_2}(T)$ (kg l^{-1}) extracted from REFPROP 10.0 at temperature T (K):

$$\dot{m}_{H_2} = \dot{V}_{H_2}(T) \cdot \rho_{H_2}(T). \quad (2)$$

The degree of hydrogenation $DoH(t)$ is defined as the ratio of the amount of hydrogen reversibly bound to the LOHC, n_{H_2} (mol), divided by the maximum reversible hydrogen storage capacity of the H0-DBT / H18-DBT system $n_{H_2,max}$ (mol) [17]. The maximum storage capacity of our system is 6.2 mass % as mentioned above. For the experiments reported in this contribution, the $DoH(t)$ can be derived from

$$DoH(t) = DoH(t_0) - \frac{\int_{t_0}^{t} \dot{n}_{H_2,reaction}(t)dt}{n_{H_2,max}}. \quad (3)$$

The hydrogen flow rate $\dot{n}_{H_2,reaction}$ (mol s^{-1}) is determined by flow measurements. Hydrogen volume flow measurements were conducted at ambient pressure and known temperature. The ideal gas law was applied. The maximum amount of stored hydrogen $n_{H_2,max}$ (mol) is defined by the amount of LOHC in the system and the stoichiometry.
The output of the dehydrogenation reaction is quantified by the hydrogen yield Y_{H_2}, which is defined as the ratio between the released hydrogen (mol) and the hydrogen initially stored (mol) over a time period Δt (s). The hydrogen yield is calculated by

$$Y_{H_2} = \frac{n_{H_2,reaction}}{n_{H_2,initial}} \quad (4)$$

Productivity is a value to quantitatively compare hydrogen release rates for different boundary conditions. The productivity P (g_{H2} g_{Pt}^{-1} min^{-1}) is defined as the mass of released hydrogen Δm_{H_2} (g) over a period of time Δt (s) per mass of platinum m_{Pt} (g) in the catalyst [17]:

$$P = \frac{\Delta m_{H_2}}{m_{Pt} \cdot \Delta t} \quad (5)$$

Productivity and hydrogen yield are evaluated over a period with constant boundary conditions.

2.4. Gas chromatographic analysis to detect side product formation

Based on a publication by Jorschick et al. [29], gas chromatographic analysis was used to separate DBT species from low-boiling (LB) and high-boiling (HB) impurities and determine sample composition. The approach for the distinction between various Hx-DBT isomers follows that of Dürr et al. [61]; a gas chromatograph Agilent 8860 GC equipped with a capillary column (DB-225MS, Agilent Technologies) was used to separate Hx-DBT isomers. The temperature program of the chromatographic method used to analyze sample composition is shown in Table 2.

Table 2: Temperature program of the chromatographic method used to analyse sample composition. Flow conditions: 1:150 split injection, 1.2 ml min^{-1} helium at constant column flow at 250°C injector temperature.

Parameters			
Step	Heating rate / °C min^{-1}	Temperature / °C	Hold time / min
1	11	130	3.5
2	11	170	3.5
3	5	185	11
4	3	190	7
5	3	195	8
3	3	200	4
7	20	210	50

3. Results and discussion

3.1. Overview of the results of a measurement day

The dehydrogenation experiments were performed with different H18-DBT flow rates and different average temperatures in the dehydrogenation unit, as shown in Table 1. The pressure was constant at 2 bar (absolute) during the experiments. In an additional measurement, an absolute pressure variation between 1.6 bar and 3.3 bar was performed with the same parameters as in exp. 5 (see Table 1). Figure 5 shows the influence of the variation of the LOHC mass flow on the resulting hydrogen mass flow in (a) and on the different temperatures in the dehydrogenation unit in (b) during the same measurement day. In (c), the corresponding thermal load of the burner and the hydrogen production rate calculated according to Equation (1) are plotted.
During the measurement campaign, a total of seven measurement days were carried out, as illustrated as an example in Figure 5. The experiment shown in Figure 5 starts with the cold start of the LOHC dehydrogenation unit at an ambient temperature of about 23°C. The temperatures shown in Figure 5 (b) represent those of the exhaust gas before (ϑ_{bD}) and after (ϑ_{aD}) the fixed bed reactor and the average temperatures inside the fixed bed reactor, ϑ_{mD}, (see Section 2.2). The resulting hydrogen mass flow (see Figure 5 (a) and (b)) is calculated using Equation (2) and the measured hydrogen volume flow averaged over a 200 s time interval. The burner was initially operated at full load (3.0 kW) during the cold start of the system. The PID controller automatically reduced the thermal load of the burner after the set temperature was reached in the fixed bed reactor until the system achieved steady state. Due to the wide power modulation range of the porous media burner, the dehydrogenation unit achieves the reaction temperature quickly (about 25 minutes) and the hydrogen release reaction starts about 30 min after the system cold start (see Figure 5). This is in contrast to systems with alternative heating concepts described in the literature, where it takes far more than 60 minutes for the hydrogen release reaction to start [32, 39].

Figure 5 clearly shows the transient response of the measured quantities after parameter adjustment for the respective measurement point. Since this process takes up to 45 min, the evaluation of the measured data is performed in the last 30 min of an individual measurement point (grey-shaded area).

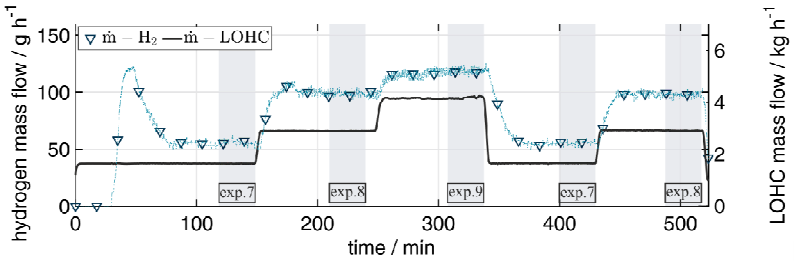

(a) LOHC input mass flow and resulting hydrogen mass flow

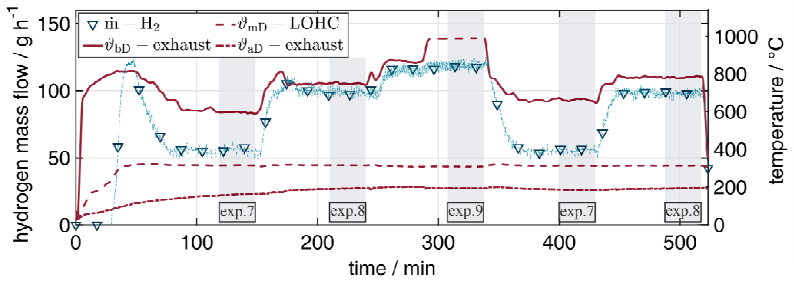

(b) Temperatures in the dehydrogenation unit and resulting hydrogen mass flow

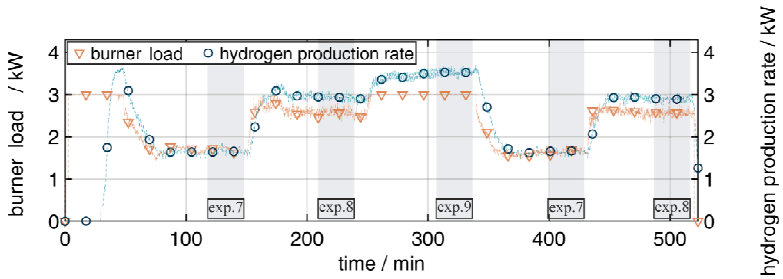

(c) Calculated thermal load of the burner during dynamic operation and corresponding hydrogen production rate (related to lower heating value)

Figure 5: General overview of the measurement results of exp.7, exp.8 and exp.9 (see Table 1) during a measurement day including heat-up times and repetitions of the individual measurement points. Time intervals relevant for the evaluation are highlighted in grey and marked with the name of the respective measurement point. Temperatures shown in Figure 5 (b) represent those of the exhaust gas before (ϑ_{bD}) and after (ϑ_{aD}) the fixed bed reactor and the average temperatures inside the fixed bed reactor, ϑ_{mD}.

All measurement points listed in Table 1 were processed as described above. In Fig. 5, an example of the performance of the system for exps. 7, 8, and 9 is shown. During these experiments, the average temperature inside the fixed bed reactor ϑ_{mD} was constant at 320°C (see Fig. 5 (b)), and the H18-DBT mass flow was increased from 1.6 kg h^{-1} to 2.9 kg h^{-1} to 4.2 kg h^{-1}, followed by the repetition of the first two H18-DBT mass

flows of 1.6 kg h^{-1} and 2.9 kg h^{-1} (see Fig. 5 (a)). In this way, it is shown that the trends of the individual experiments are reproducible and independent on the sequence of, for example, the mass flow variation. Both repeated experiments 7 and 8 demonstrate very similar results, respectively. The resulting temperatures of the exhaust gas before the fixed-bed reactor (ϑ_{bD}, red curve) reach a value of about 800°C after ignition of the burner, since the system is at 23°C and the porous media burner is operated at full load of 3.0 kW (see Fig. 5 (c)). After reduction of the burner thermal load to about 1.8 kW during exp. 7, ϑ_{bD} reduces to about 600°C followed by a rise in temperature to over 1000°C during exp. 9 at full burner load of 3.0 kW. For exp. 9, the exhaust gas temperature prior to the fixed bed reactor is even higher than 1000°C, however, this temperature is beyond the measurement range of the thermocouple and therefore is not recorded (reason for the dashed line at exp. 9 in Fig. 5). The exhaust gas temperature after the fixed bed reactor (ϑ_{aD}, red dash-dotted line) is nearly constant after the heat-up phase and reaches a maximum of about 200°C once the system has reached steady state. For a range between 0.6 kW and 3.0 kW of thermal load, the resulting exhaust gas volume flows are between $0.9 \cdot 10^{-3}$ m^3 s^{-1} and $3.2 \cdot 10^{-3}$ m^3 s^{-1} and the residence time of the exhaust gas is about 2.4 s to 0.6 s. Comparing the temperatures before (ϑ_{bD} ranged from 600°C to over 1000°C) and after (ϑ_{aD} reaches a maximum of about 200°C) the fixed bed reactor and those in the dehydrogenation volume (ϑ_{mD} with a nearly constant level of 320°C in the case shown), the enthalpy present in the exhaust gas flow is transferred very effectively to the dehydrogenation reaction. The increase in exhaust gas temperatures ϑ_{bD} between exp. 7 and 9 results from the increase in thermal load by higher LOHC mass flows and thus, increased heat demand of the endothermic reaction in the fixed bed reactor (see Figs. 5 (a), (b), and (c)). In general, it is found that due to the good heat transfer from the exhaust gas to the dehydrogenation reaction caused by the dynamic burner operation, a change in LOHC mass flow (black line in Fig. 5 (a)) leads to a rapid change in hydrogen mass flow (blue dotted line in Fig. 5). It only takes between 10 to 20 minutes to reach a new steady-state level. For a temperature in the reaction zone of 320°C and an H18-DBT mass flow of 1.6 kg h^{-1}, a hydrogen mass flow of about 56 g h^{-1} is achieved. Increasing the LOHC mass flow to 4.2 kg h^{-1} results in a hydrogen mass flow of 119 g h^{-1} (blue dotted line in Fig. 5 (a)). The estimated average residence time of the H18-DBT in our fixed bed reactor is about 190 min for a mass flow of 1.6 kg h^{-1} and about 75 min for a mass flow of 4.2 kg h^{-1}. The values of the hydrogen mass flow correspond to a hydrogen production rate according to Equation (1) of about 1.9 kW for the lower H18-DBT mass flow and of about 3.9 kW for a LOHC mass flow of 4.2 kg h^{-1} (blue dotted line in Fig. 5 (c)). The overall efficiency of the system is addressed in detail for selected measurement points at the end of chapter 3.2. In our setup, increasing the LOHC mass flow by a factor of 2.5 results in an increase of the hydrogen production rate by a factor of two. This increase in hydrogen release is due to the higher amount of fully hydrogenated H18-DBT and a higher intermediate DoH in the reaction volume. A likely reason for the just doubled hydrogen production rate is the shorter residence time of the LOHC in the dehydrogenation unit at a higher LOHC mass flow. Overall, our dehydrogenation system achieved heating rates of about 10 K min^{-1} and a temporal change rate of the hydrogen release when boundary conditions of the reaction are varied of about 6 g_{H2} min^{-1}, demonstrating the dynamic nature of our burner-heated dehydrogenation system. Compared to our previous burner heated system [55], these values are lower by a factor six to nine, but relative to its size, the system is still highly dynamic.

The first peak of the hydrogen mass flow at about 45 minutes after the cold start of the dehydrogenation unit results from the existing large mass of H18-DBT in the reaction volume at this time, since the fixed bed reactor is continuously flushed with H18-DBT during the cooling and heating process. During these processes, however, the temperature in the reaction volume is too low for a hydrogen release reaction. As soon as a temperature is reached, that is sufficiently high for hydrogen release, a large amount of H18-DBT is suddenly dehydrogenated, resulting in the peaks shown in Figures 5 and 6. In the further progress, only the H18-DBT freshly pumped into the dehydrogenation unit is dehydrogenated and the hydrogen mass flow returns to a steady level.

Figure 6 shows in detail the mean temperature in the reaction volume (ϑ_{mD}-LOHC, red line) as well as the respective minimum and maximum temperatures (red shaded area) in the release unit, plotted for the same experiment as shown in Figure 5. The given minimum and maximum temperatures indicate the span of the

temperatures recorded by the thermocouples (TI 06 – TI 17) within the reaction volume. In addition, the resulting hydrogen production rate (blue curve) and the degree of hydrogenation (orange line) are shown. The mean and target temperature in the reaction volume shows a nearly constant value of 320°C. Only in the case of parameter changes between the individual experiments small deviations become visible. An exception is exp. 9, since the burner with its maximum load of 3.0 kW could not ensure a sufficient heat supply for the hydrogen release reaction under the given boundary conditions, the mean temperature dropped to approx. 312°C. Due to the size of the fixed bed reactor a temperature spread within the reaction volume in a range of about 20 K (red shaded area) can be observed. As mentioned before, we achieved hydrogen production rates between 1.9 kW and 3.9 kW. The upper value is limited by the lower temperature in the reaction volume, which results from the limitation of the burner power.

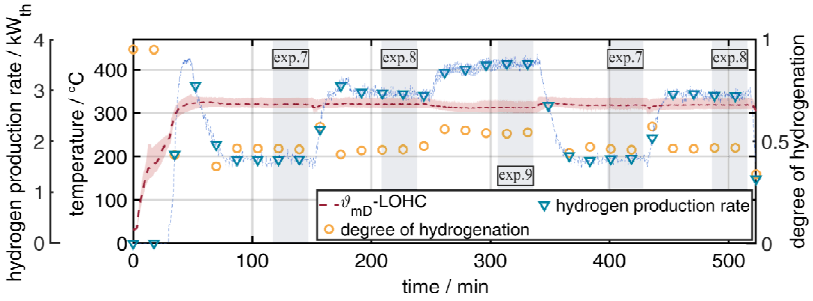

Figure 6: Degree of hydrogenation, hydrogen production rate and temperature distribution inside the burner-heated dehydrogenation unit for operation with an increasing H18-DBT mass flow from 1.6 kg h^{-1} to 4.2 kg h^{-1}. Conditions: set reaction temperature: 320°C; pressure 2 bar (absolute); dynamic operation of the burner load between 0.6 kW and 3.0 kW.

The degree of hydrogenation (orange line in Fig. 6) is nearly constant at about 46 % for LOHC mass flows of 1.6 kg h^{-1} and 2.9 kg h^{-1} but increases at the higher LOHC mass flow of 4.2 kg h^{-1} as a smaller proportion of stored hydrogen is released due to the lower temperature in the reaction volume. As demonstrated, about 54 % of the stored hydrogen was released in exps. 7 and 8, but only 46 % was released in exp. 9 for the highest LOHC mass flow (see Fig. 6). In other words, from the original 6.2 mass % of hydrogen stored in the LOHC, about 3.7 mass % are released at LOHC mass flows of 1.6 kg h^{-1} and 2.9 kg h^{-1}, and about 2.9 mass % are released at a LOHC mass flow of 4.2 kg h^{-1}. An increase in the amount of hydrogen released could be achieved by increasing the residence time of the H18-DBT in the fixed bed reactor, which can be obtained by a larger reaction volume or by recycling the LOHC product to the dehydrogenation unit at the expense of a lower hydrogen production rate. In general, the results show a very dynamic behavior of our release unit compared to existing systems [32, 39] as a result of the dynamic operation of the porous media burner and the efficient heat transfer from the exhaust gas to the reaction volume. An overall result is that exhaust gas temperature and residence time of the LOHC in the reaction volume appear to have a significant effect on the hydrogen release and thus on the hydrogen production rate and degree of hydrogenation, which is in agreement with the literature [29, 33, 55, 61].

Throughout the measurement days, an additional exhaust gas analysis was performed during the start-up process and continuous operation. The results showed that apart from the burner ignition period (here H_2: 300 ppmV and CO: 580 ppmV) no significant H_2 and CO emissions were generated. The combined NO_2 and NO emissions were nearly constant at about 38 ppmV and comply with existing emission standards. The results also agree well with those shown in [55], where a similar burner was used.

With the experiments shown, we have demonstrated for the first time that when a porous media burner in combination with an appropriately designed fixed bed reactor is used, very dynamic hydrogen release from H18-DBT is possible at a kW scale. Consequently, in the following section, the hydrogen release behavior

under various process conditions and the system efficiency of our dehydrogenation system are investigated in more detail.

3.2. LOHC dehydrogenation under various boundary conditions

In this section, the influence of the following parameters on the resulting hydrogen mass flow is further analyzed:

- the LOHC feed mass flow and the residence time of the LOHC in the reaction volume;
- the temperature level of the reaction in the dehydrogenation unit, which is determined by the burner load;
- the pressure level in the dehydrogenation unit (separate case study).

The results of the parameter variations for the measurement points shown in Table 1 are summarized in Table 3.

Table 3: Overview of the results of the experiments.

	Parameters						
Experiment	Temperature / °C	Mass flow LOHC / kg h^{-1}	Pressure / bar (absolute)	Hydrogen mass flow / g h^{-1}	Productivity / g_{H2} min^{-1} g_{Pt}^{-1}	Hydrogen production rate / kW	DoH det. by Equ.(3) / %
exp.1	282	1.6	2.0	23.9	0.1	0.8	74
exp.2	283	2.9	2.1	40.7	0.2	1.4	75
exp.3	286	4.2	2.1	58.3	0.3	1.9	75
exp.4	302	1.6	1.9	46.3	0.2	1.5	57
exp.5	304	2.9	2.0	76.8	0.4	2.6	57
exp.6	306	4.2	2.0	92.7	0.5	3.1	56
exp.7	319	1.6	1.8	55.7	0.3	1.9	46
exp.8	320	2.9	1.9	98.2	0.5	3.2	46
exp.9	312	4.2	2.0	118.5	0.6	3.9	54

The measurement points were recorded according to the procedure described in Section 3.1. Due to the adjustments of the PID-controller, the burner was operated with a deviation of about 10 % after completion of the heating process (see also Fig. 5), while the fluctuation of the mean temperature in the reaction volume was less than ± 5.0 %. The error bars shown in Fig. 7 and Fig. 8 indicate the span between individual measurement runs for an experiment with identical boundary conditions.
During the first two days of operation of the dehydrogenation unit, catalyst degradation of about 30 % was observed. This is in agreement with the literature according to which degradation is seen in the first 10 to 20 hours of operation and the catalyst subsequently stabilizes at an almost constant level [62]. Since the experiments shown were performed after the dehydrogenation unit had been in operation for three days, the degradation of the catalyst has no significant effect on the results shown below.
Figure 7 shows the influence of increasing the temperature from about 284°C to about 319°C and the LOHC mass flow from 1.6 kg h^{-1} to 4.2 kg h^{-1} and thus of reducing the residence time on the hydrogen mass flow, the hydrogen yield and the resulting catalyst productivity.
As expected, the reaction rate of the hydrogen release reaction is higher at a higher temperature and a higher LOHC mass flow rate, resulting in increased hydrogen mass flows. A higher temperature has a positive effect on the thermodynamic driving force and the reaction kinetics of the dehydrogenation reaction [33, 39, 62]. A higher LOHC mass flow results in a higher intermediate degree of hydrogenation within the reaction volume increasing the overall reaction rate [33]. In our case, a temperature increase of about 20 K leads to an increase of the hydrogen mass flow between about 20 % and 100 %, depending on the level of the LOHC mass flow. An increase in LOHC mass flow of about 1.3 kg h^{-1} results in an increase of hydrogen mass flow between about

20 % and 80 %, depending on the temperature level in the fixed bed reactor. As shown in Table 3, the resulting average DoH of each of the experiments displayed is between 46 % and 75 %. For the variation of the LOHC mass flows at a constant reaction temperature, there is a slight increase in the resulting DoH. However, an increase in the reaction temperature from approx. 280°C to approx. 320°C leads to a strong decrease in the DoH from approx. 75 % to approx. 46 %. At a higher reaction temperature, 29 % more of the stored hydrogen is thus released.

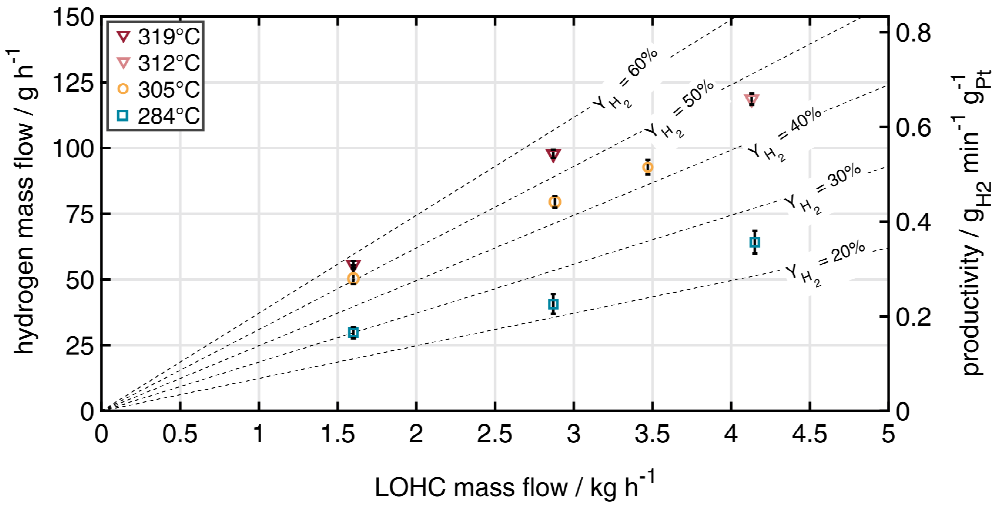

Figure 7: Hydrogen yield and catalyst productivity of the burner-heated dehydrogenation unit with increasing H18-DBT mass flow from 1.6 kg h^{-1} to 4.2 kg h^{-1} and with an increasing average temperature in the reaction volume between 284°C and 319°C for a constant pressure of 2 bar (absolute).

Since we achieve sufficient temperature for the dehydrogenation process over the whole dehydrogenation unit, the entire 1000 g (0.3 mass % Pt on alumina) of catalyst were considered for the calculation of productivity. In general, catalyst productivity and hydrogen yield increase also with higher H18-DBT mass flow and temperature in the fixed bed reactor. Since we only reached a maximum temperature of 312°C in the reactor for the highest LOHC mass flow due to the maximal burner thermal load, this measurement point was added in Figure 7 in the form of a separate temperature point (light red). Figure 7 shows, on the one hand, that for all temperature levels the hydrogen yield decreases slightly with increasing LOHC mass flow. This can be attributed to the shorter residence time of the loaded H18-DBT at the catalyst with increasing LOHC mass flow. On the other hand, an increase in temperature at a low LOHC mass flow leads to a smaller increase in hydrogen yield compared to the case of a high LOHC mass flow. This behavior can be explained by a lower intermediate DoH at a low LOHC mass flow, which kinetically and thermodynamically limits the possibility of increasing the hydrogen yield with higher temperatures. Overall, a catalyst productivity of maximum 0.65 g_{H_2} min^{-1} g_{Pt}^{-1} (312°C, H18-DBT flow rate: 4.2 kg h^{-1}) was achieved for a release of 46 % of the stored hydrogen. In comparison, for similar boundary conditions a productivity of 0.7-1.2 g_{H_2} min^{-1} g_{Pt}^{-1} was realized by Jorschick et al.[17] for release of 40 % of the stored hydrogen. Mrusek et al. realized 0.17 g_{H_2} min^{-1} g_{Pt}^{-1} for a lower pressure of 1 bar (absolute) and a reaction temperature of 260°C and Wunsch et al. [30] showed a productivity of 1.1 g_{H_2} min^{-1} g_{Pt}^{-1} for a similar temperature level but lower hydrogen yield. Under consideration of the reaction volume of 7.3 l, we reached a power density of the dehydrogenation unit of 0.5 kW_{therm} l^{-1}. Since the reaction volume is currently only half filled with catalyst and the performance of the burner is insufficient for higher hydrogen mass flows, a significant increase in power density and productivity is possible with the

existing setup when more catalyst material or a more powerful burner is used in future studies.
The influence of a pressure variation between 1.6 bar (absolute) and 3.3 bar (absolute) was carried out with the same parameters as in exp. 5 (see Table 1) and the results are shown in Figure 8. In the pressure variation study an average temperature level in the reaction volume of about 304°C and a LOHC mass flow rate of 2.9 kg h^{-1} were applied. For the experiments shown in Figure 8, the DoH was in the range between 57 % and 61%.

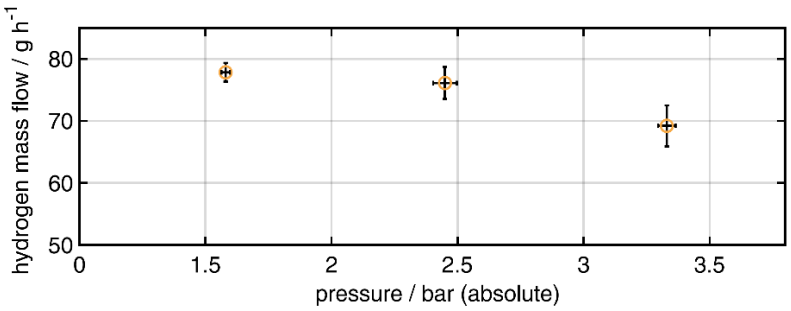

Figure 8: Hydrogen mass flows for operation of the burner-heated dehydrogenation unit with a pressure level between 1.6 bar (absolute) and 3.3 bar (absolute). Conditions: H18–DBT mass flow: 2.9 kg h^{-1}; average temperature in the reaction volume about 304°C.

As can be seen from the results, an increasing pressure level leads to a decrease in hydrogen release, being in accordance with observations in literature [33]. A doubling of the pressure in the reaction volume leads to a decrease in the hydrogen mass flow by about 12 %. In conclusion, however, the influence of an increase in pressure in the reaction volume is small compared to the residence time of the LOHC in the dehydrogenation unit and the existing temperature level.
In our further studies an energetic analysis of the system was carried out with regard to the overall efficiency. Table 4 gives an overview of the energy balance of the respective experiments, represented by the electricity demand of the setup (e.g. for the pumps, the controller and the measurement equipment), the burner load and the hydrogen production rate of the individual experiments.

Table 4: Energetic overview of the experiments.

	Parameters			
Experiment	Electricity demand of the setup / kW	Burner load / kW	Power demand of setup / kW	Hydrogen production rate / kW
exp.1	0.15	1.04	1.19	0.8
exp.2	0.15	1.55	1.70	1.4
exp.3	0.15	1.95	2.10	1.9
exp.4	0.15	1.49	1.64	1.5
exp.5	0.15	2.15	2.30	2.6
exp.6	0.15	2.51	2.66	3.1
exp.7	0.15	1.69	1.84	1.9
exp.8	0.15	2.56	2.71	3.2
exp.9	0.15	3.00	3.15	3.9

The electricity demand of the system is constant at about 0.15 kW for all experiments. The reported energy demand of the setup is the sum of the electricity demand and the respective burner load. As shown, when the hydrogen production rate exceeds 1.9 kW, the system has a higher energetic output than input. This boundary is probably due to energy losses to the environment, which have a more significant impact downstream. For

even larger systems, this energy loss could potentially be reduced significantly, since the impact of heat losses to the environment decreases, relative to the reaction heat demand. At its best point in experiment 9, the overall efficiency is about 24 %. This means that the released hydrogen has an energy content, that is 24 % higher than the energy required to achieve its release. Compared with values from the literature, according to which a theoretical overall efficiency of about 70 % could be achieved [16], there is certainly potential for improvement, e.g. by applying better heat insulation. However, compared to the authors' previous work, studying a small-scale dehydrogenation unit [55], the overall efficiency shown is a big step towards the values achievable in theory. Additionally, the theoretical efficiency refers to the release reaction in the reaction volume and not to a complete dehydrogenation system such as in the given scenario.

3.3. LOHC degree of hydrogenation (DoH) and side product formation

In this section, the resulting degree of hydrogenation, the amount of Hx-DBT isomers, and the resulting by-products are analyzed using one sample each from exps. 1, 4 and 7. Carbon nuclear magnetic resonance spectroscopy (^{13}C-NMR) was used to determine the degree of hydrogenation (DoH), using LOHC sample preparation and measuring conditions as recently published by Dürr et al. [61]. A comparison of the resulting values for DoH with measurements of the refractive index (using a DR6100-T (A. Kruss Optronic GmbH)) [62] and calculations according to Equation 3 are shown in Table 5.

Table 5: Comparison of DoH determined by measurements of ^{13}C-NMR and refractive index of selected samples before and after dehydrogenation of H18-DBT.

	Parameters		
Experiment	DoH det. by ^{13}C-NMR / %	DoH det. by refractive index / %	DoH det. by Equ. (3) / %
exp.1	77.9	77.4	79.2
exp.4	56.8	56.3	57.9
exp.7	33.8	28.2	46.1
H18-DBT	100.0	100.7	-

The evaluation of the DoH according to both methods show high agreement for all samples. The accuracy of the correlation between degree of hydrogenation and refractive index decreases with descending DoH. The DoH calculated according to Eq. 3 also shows high agreement for large DoH, but deviates for the experiment with a low concentration. This effect occurs reproducibly and can either be attributed to density stratification in the sampling process or has its cause in the different evaporation behavior of the various DBT species.
Figure 9 shows the chromatogram of a representative Hx-DBT mixture (experiment 4) after the dehydrogenation of fully hydrogenated H18-DBT. Apart from low and high boiling by-products, the categorization of the different Hx-DBT isomers H18-DBT (23-31 min retention time), H12-DBT (32-42 min retention time), H6-DBT (43-57 min retention time) and H0-DBT (58-72 min retention time) can be seen. According to the gas chromatographic analysis, all species of Hx-DBT, including the partially dehydrogenated components H6-DBT and H12-DBT, are present in the product mixtures. In the example of experiment 4, ratios of 32 % and 39.6 % were observed for the partially dehydrogenated H6-DBT and H12-DBT, respectively. In the same sample 7.7 % of the Hx-DBT species was fully dehydrogenated, whereas 20.7 % of the H12-DBT were not dehydrogenated at all, leading to a degree of hydrogenation of the mixture of approx. 57 %. This simultaneous occurrence of partially and fully dehydrogenated LOHC indicates a rather ideal residence time distribution in the reactor. Therefore, a relatively uniform distribution of the LOHC flow in the reaction volume without liquid by-pass flows can be derived from these results. In contrast, with a relatively fast flow through the reaction volume, a large amount of barely dehydrogenated Hx-DBT should be expected. Based on these results, a uniform hydrogen release and a homogeneous flow distribution without recirculation zones can be assumed.

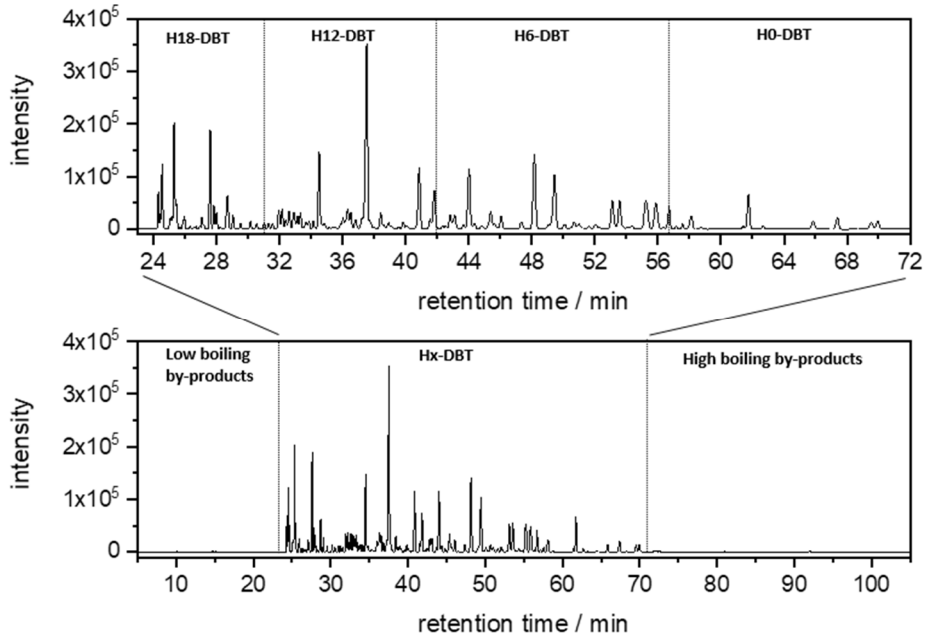

Figure 9: Chromatogram of a Hx-DBT mixture (experiment 4) after dehydrogenation of H18-DBT.

To interpret the formation of side-products, the proportions of high boiling and low boiling substances (relative to the boiling points of Hx-DBT) are examined. Table 6 summarizes the composition of selected samples before and after dehydrogenation of H18-DBT.

Table 6: Composition of the selected samples from Experiment 1, 4, and 7 after dehydrogenation of H18-DBT and composition of H18-DBT before dehydrogenation.

	Parameters		
Experiment	High boilers / wt.-%	Low boilers / wt.-%	Hx-DBT / wt.-%
exp. 1	0.2	0.2	99.6
exp. 4	0.5	0.3	99.2
exp. 7	0.6	0.9	98.5
H18-DBT	0.0	0.2	99.8

First it should be emphasized, that the feed samples already show traces of low boiling species in the range of 0.2 wt.-%, respectively, prior to the dehydrogenation experiments. The amount of high and low boiling components in the samples with still high DoH, are in the same order of magnitude as the initial feed composition. Therefore, only slightly dehydrogenated samples show no significant side-product formation, whereas the sample from exp. 7 contains 0.6 wt.-% of high boilers and 0.9 wt.- % of low boilers. Dehydrogenation conditions that lead to lower DoH, due to enhanced hydrogen release, also promote the formation of side-products. Nevertheless, the amount of side products formed in the herein used reactor is in the range of similar dehydrogenation setups mentioned in prior publications [29].

4. Conclusion and outlook

In this publication, we demonstrated for the first time a kW-scale LOHC dehydrogenation process thermally driven by the exhaust gas enthalpy of a porous media burner. We focused on the experimental investigation of a heating concept with which we optimized the heat input into the dehydrogenation unit, the power density and the overall efficiency. Our dehydrogenation unit, consisting of the burner and the fixed-bed reactor, proved to be very efficient in transferring heat, which resulted in good system dynamics. The biomethane-fueled porous media burner was operated between 0.6 kW and 3.0 kW and exhibited low pollutant emissions. However, it should be noted that the availability of biomethane might vary.
A LOHC temperature spread was observed within the reaction zone in a range of about 20 K, which was independent on the H18-DBT mass flow rate and can be attributed to the size of the fixed-bed reactor (internal volume 7.3 l). For a LOHC mass flow rate of 1.6 kg h^{-1} the estimated residence time was about 190 min and for a mass flow rate of 4.2 kg h^{-1} this value amounted to about 75 min. The hydrogen release reaction starts about 30 min after the system cold start. This is in significant contrast to indirectly heated systems of comparable size described in the literature, where it takes more than 60 minutes for the hydrogen release reaction to start [32, 39]. Our dehydrogenation system achieved heating rates of about 10 K min^{-1} demonstrating the dynamic nature of our burner-heated dehydrogenation system. At a LOHC mass flow rate of 4.2 kg h^{-1}, a maximum output power based on the lower heating value of hydrogen of about 3.9 kW was achieved. Considering the fixed bed volume, a power density of about 0.5 kW_{therm} l^{1} could be reached. A maximum catalyst productivity of 0.65 g_{H2} min^{-1} g_{Pt}^{-1} (312°C, H18-DBT flow rate: 4.2 kg h^{-1}) was achieved for a degree of hydrogenation of 54%, which is comparable to existing systems that, however, have a lower hydrogen production rate [29]. A significant increase in power density and productivity should be possible with the existing setup and more catalyst material or with a more powerful burner.
An increase in LOHC mass flow of about 1.3 kg h^{-1} results in an increase of hydrogen mass flow between about 20 % and 80 %, depending on the temperature level in the fixed bed reactor. A similar behaviour was observed for the hydrogen mass flow when the reaction temperature increased, while a doubling of the pressure in the reaction volume leads to a decrease in the hydrogen mass flow by about 12 %. A maximum overall system efficiency of 24 % was achieved, relating the lower heating value of the hydrogen released to the total energy input, which is governed by the enthalpy of the fuel, includes all heat losses and also comprises the electrical energy required for the operation of the system. Additionally, the amount of by-products formed in the reactor used here is in the order of magnitude of similar dehydrogenation plants mentioned in previous publications, although the heat here is applied very directly [29].
The reported dynamic range and power density values of direct burner heated dehydrogenation systems make them attractive for a wide range of applications. Especially in the context of the accelerated establishment of a network of hydrogen refuelling stations (HRS) for mobile applications, the described burner-heated dehydrogenation unit is a good opportunity to use the infrastructure currently available at refuelling stations (e.g. available methane) to provide hydrogen. Future research and development will focus on improving the power density and catalyst productivity of the dehydrogenation system mentioned here by using more catalyst in the reaction volume and a more powerful burner. A very attractive extension towards even higher burner power and cleaner operation is of course the use of hydrogen as burner fuel instead of methane. In addition, potential sources of heat losses to the environment should be identified and avoided to improve the overall efficiency of the dehydrogenation system.

Acknowledgment

We acknowledge support by the Bavarian Ministry of Economics, in particular through funding of the Energy Campus Nürnberg (EnCN). Furthermore, we thank our colleagues and participating students at LTT, in particular Thomas Dressel, Peter Demmelmeyer, Nikolas Schmidt, Marcel Müller, and Lars Gerboth for supporting realization of the system and the measurements, respectively.

Nomenclature

		n_{H_2}	hydrogen storage capacity
		N_2	nitrogen
Al_2O_3	alumina	NEC	N-ethylcarbazol
CO	carbon monoxide	NO_2	nitrogen dioxide
CO_2	carbon dioxide	NO_X	nitric oxide
CW	cooling water	P_{H_2}	hydrogen productivity
^{13}C-NMR	carbon nuclear magnetic resonance spectroscopy	P_{burner}	thermal load of the burner
DBT	dibenzyltoluene	PEM	proton exchange membrane
DoH	degree of hydrogenation	PI	pressure indicator
HB	high-boiling	PID	proportional integral derivative controller
H_2	hydrogen	PLC	programmable logic controller
H0-DBT	dibenzyltoluene	Pt	platinum
H18-DBT	perhydro dibenzyltoluene	SiSiC	Silicon infiltrated silicon carbide
HRS	hydrogen refuelling station	TI	temperature indicator
IC	internal combustion	ϑ_{bD}-exhaust	temperature before the dehydrogenation unit
LB	low-boiling	ϑ_{aD}-exhaust	temperature after the dehydrogenation unit
LHV_{H_2}	lower heating value of hydrogen	ϑ_{mD}-LOHC	medium temperature in the dehydrogenation unit
LOHC	liquid organic hydrogen carrier	$\dot{V}_{H_2}(\vartheta)$	hydrogen volume flow
MFC	mass flow controller	Y_{H_2}	hydrogen yield
MFM	mass flow meter	$\rho_{H_2}(\vartheta)$	hydrogen density
$\dot{m}_{H_2}$	hydrogen mass flow		

References

[1] Tremel A, Wasserscheid P, Baldauf M, Hammer T. Techno-economic analysis for the synthesis of liquid and gaseous fuels based on hydrogen production via electrolysis. International Journal of Hydrogen Energy. 2015;40:11457-64.
[2] Fonseca JD, Camargo M, Commenge J-M, Falk L, Gil ID. Trends in design of distributed energy systems using hydrogen as energy vector: A systematic literature review. International Journal of Hydrogen Energy. 2019;44:9486-504.
[3] Runge P, Sölch C, Albert J, Wasserscheid P, Zöttl G, Grimm V. Economic comparison of different electric fuels for energy scenarios in 2035. Applied Energy. 2019;233-234:1078-93.
[4] Hänggi S, Elbert P, Bütler T, Cabalzar U, Teske S, Bach C, et al. A review of synthetic fuels for passenger vehicles. Energy Reports. 2019;5:555-69.
[5] Knosala K, Kotzur L, Röben FTC, Stenzel P, Blum L, Robinius M, et al. Hybrid Hydrogen Home Storage for Decentralized Energy Autonomy. International Journal of Hydrogen Energy. 2021;46:21748-63.
[6] Preuster P, Papp C, Wasserscheid P. Liquid Organic Hydrogen Carriers (LOHCs): Toward a Hydrogen-free Hydrogen Economy. Acc Chem Res. 2017;50:74-85.
[7] Reuß M, Grube T, Robinius M, Preuster P, Wasserscheid P, Stolten D. Seasonal storage and alternative carriers: A flexible hydrogen supply chain model. Applied Energy. 2017;200:290-302.
[8] Aakko-Saksa PT, Cook C, Kiviaho J, Repo T. Liquid organic hydrogen carriers for transportation and storing of renewable energy – Review and discussion. Journal of Power Sources. 2018;396:803-23.
[9] Wulf C, Zapp P, Schreiber A. Review of Power-to-X Demonstration Projects in Europe. Frontiers in Energy Research. 2020;8.
[10] Noh H, Kang K, Seo Y. Environmental and energy efficiency assessments of offshore hydrogen supply chains utilizing compressed gaseous hydrogen, liquefied hydrogen, liquid organic hydrogen carriers and ammonia. International Journal of Hydrogen Energy. 2023;48:7515-32.
[11] Seo Y, Park H, Lee S, Kim J, Han S. Design concepts of hydrogen supply chain to bring consumers offshore green hydrogen. International Journal of Hydrogen Energy. 2023.
[12] Usman MR. Hydrogen storage methods: Review and current status. Renewable and Sustainable Energy Reviews. 2022;167:112743.
[13] Zivar D, Kumar S, Foroozesh J. Underground hydrogen storage: A comprehensive review. International Journal of Hydrogen Energy. 2021;46:23436-62.
[14] Rong Y, Chen S, Li C, Chen X, Xie L, Chen J, et al. Techno-economic analysis of hydrogen storage and transportation from hydrogen plant to terminal refueling station. International Journal of Hydrogen Energy. 2023.
[15] Preuster P, Alekseev A, Wasserscheid P. Hydrogen Storage Technologies for Future Energy Systems. Annual review of chemical and biomolecular engineering. 2017;8:445-71.
[16] Preuster P, Fang Q, Peters R, Deja R, Nguyen VN, Blum L, et al. Solid oxide fuel cell operating on liquid organic hydrogen carrier-based hydrogen – making full use of heat integration potentials. International Journal of Hydrogen Energy. 2018;43:1758-68.
[17] Jorschick H, Preuster P, Dürr S, Seidel A, Müller K, Bösmann A, et al. Hydrogen storage using a hot pressure swing reactor. Energy & Environmental Science. 2017;10:1652-9.
[18] Teichmann D, Arlt W, Wasserscheid P. Liquid Organic Hydrogen Carriers as an efficient vector for the transport and storage of renewable energy. International Journal of Hydrogen Energy. 2012;37:18118-32.
[19] Aslam R, Khan MH, Ishaq M, Muller K. Thermophysical Studies of Dibenzyltoluene and Its Partially and Fully Hydrogenated Derivatives. J Chem Eng Data. 2018;63:4580-7.
[20] Teichmann D, Arlt W, Wasserscheid P, Freymann R. A future energy supply based on Liquid Organic Hydrogen Carriers (LOHC). Energy & Environmental Science. 2011;4.
[21] Kim C, Cho SH, Cho SM, Na Y, Kim S, Kim DK. Review of hydrogen infrastructure: The current status and roll-out strategy. International Journal of Hydrogen Energy. 2023;48:1701-16.

[22] Rivard E, Trudeau M, Zaghib K. Hydrogen Storage for Mobility: A Review. Materials (Basel). 2019;12.
[23] Bruckner N, Obesser K, Bosmann A, Teichmann D, Arlt W, Dungs J, et al. Evaluation of industrially applied heat-transfer fluids as liquid organic hydrogen carrier systems. ChemSusChem. 2014;7:229-35.
[24] Teichmann D, Stark K, Müller K, Zöttl G, Wasserscheid P, Arlt W. Energy storage in residential and commercial buildings via Liquid Organic Hydrogen Carriers (LOHC). Energy & Environmental Science. 2012;5.
[25] Taube M, Ripplin DWT, Cresswell DL, Knecht W. A system of hydrogen-powered vehicles with liquid organic hydrides. Int J Hydrogen Energy. 1983;8:213-25.
[26] Müller K. Technologies for the Storage of Hydrogen Part 1: Hydrogen Storage in the Narrower Sense. ChemBioEng Rev. 2019;6:72–80.
[27] Müller K, Stark K, Emel'yanenko VN, Varfolomeev MA, Zaitsau DH, Shoifet E, et al. Liquid Organic Hydrogen Carriers: Thermophysical and Thermochemical Studies of Benzyl- and Dibenzyl-toluene Derivatives. Industrial & Engineering Chemistry Research. 2015;54:7967-76.
[28] Modisha P, Bessarabov D. Stress tolerance assessment of dibenzyltoluene-based liquid organic hydrogen carriers. Sustainable Energy & Fuels. 2020;4:4662-70.
[29] Jorschick H, Dürr S, Preuster P, Bösmann A, Wasserscheid P. Operational Stability of a LOHC-Based Hot Pressure Swing Reactor for Hydrogen Storage. Energy Technology. 2019;7:146-52.
[30] Wunsch A, Berg T, Pfeifer P. Hydrogen Production from the LOHC Perhydro-Dibenzyl-Toluene and Purification Using a 5 microm PdAg-Membrane in a Coupled Microstructured System. Materials (Basel). 2020;13.
[31] Do G, Preuster P, Aslam R, Bösmann A, Müller K, Arlt W, et al. Hydrogenation of the liquid organic hydrogen carrier compound dibenzyltoluene – reaction pathway determination by 1H NMR spectroscopy. Reaction Chemistry & Engineering. 2016;1:313-20.
[32] Preuster P. Entwicklung eines Reaktors zur Dehydrierung chemischer Wasserstoffträger als Bestandteil eines dezentralen, stationären Energiespeichers [Doctoralthesis]: Friedrich-Alexander-Universität Erlangen-Nürnberg (FAU); 2017.
[33] Seidel A. Entwicklung eines technischen Platin-Trägerkatalysators zur Dehydrierung von Perhydro-Dibenzyltoluol [Doctoralthesis]: Friedrich-Alexander-Universität Erlangen-Nürnberg (FAU); 2019.
[34] Wagner L. Entwicklung eines LOHC-Speicher-Systems für die stationäre Wasserstoffspeicherung im 25 kW-Maßstab [Doctoral Thesis]: Friedrich-Alexander-Universität Erlangen-Nürnberg; 2021.
[35] Modisha PM, Ouma CNM, Garidzirai R, Wasserscheid P, Bessarabov D. The Prospect of Hydrogen Storage Using Liquid Organic Hydrogen Carriers. Energy & Fuels. 2019;33:2778-96.
[36] Heublein N, Stelzner M, Sattelmayer T. Hydrogen storage using liquid organic carriers: Equilibrium simulation and dehydrogenation reactor design. International Journal of Hydrogen Energy. 2020;45:24902-16.
[37] Wunsch A, Mohr M, Pfeifer P. Intensified LOHC-Dehydrogenation Using Multi-Stage Microstructures and Pd-Based Membranes. Membranes (Basel). 2018;8.
[38] Peters W, Eypasch M, Frank T, Schwerdtfeger J, Körner C, Bösmann A, et al. Efficient hydrogen release from perhydro-N-ethylcarbazole using catalyst-coated metallic structures produced by selective electron beam melting. Energy & Environmental Science. 2015;8:641-9.
[39] Geiling J, Steinberger M, Ortner F, Seyfried R, Nuß A, Uhrig F, et al. Combined dynamic operation of PEM fuel cell and continuous dehydrogenation of perhydro-dibenzyltoluene. International Journal of Hydrogen Energy. 2021;46:35662-77.
[40] Fikrt A, Brehmer R, Milella V-O, Müller K, Bösmann A, Preuster P, et al. Dynamic power supply by hydrogen bound to a liquid organic hydrogen carrier. Applied Energy. 2017;194:1-8.
[41] Pashchenko D. Liquid organic hydrogen carriers (LOHCs) in the thermochemical waste heat recuperation systems: The energy and mass balances. International Journal of Hydrogen Energy. 2022;47:28721-9.
[42] Hampel B, Bauer S, Heublein N, Hirsch C, Sattelmayer T. Feasibility Study on Dehydrogenation of LOHC Using Excess Exhaust Heat From a Hydrogen Fueled Micro Gas Turbine. Proceedings of ASME Turbo Expo

2015. 2015:V008T23A16.
[43] Schumacher M, Mederer T, Wensing M. Investigations on a new engine concept for small hydrogen power generation units using LOHCs. SAE International: SAE International; 2013.
[44] Krieger C, Müller K, Arlt W. Coupling of a Liquid Organic Hydrogen Carrier System with Industrial Heat. Chemical Engineering & Technology. 2016;39:1570-4.
[45] Rao N, Lele AK, Patwardhan AW. Optimization of Liquid Organic Hydrogen Carrier (LOHC) dehydrogenation system. International Journal of Hydrogen Energy. 2022;47:28530-47.
[46] Badakhsh A, Song D, Moon S, Jeong H, Sohn H, Woo Nam S, et al. COX-free LOHC dehydrogenation in a heatpipe reformer highly integrated with a hydrogen burner. Chemical Engineering Journal. 2022;449:137679.
[47] Ali A, Rohini AK, Lee HJ. Dehydrogenation of perhydro-dibenzyltoluene for hydrogen production in a microchannel reactor. International Journal of Hydrogen Energy. 2022;47:20905-14.
[48] Geißelbrecht M, Mrusek S, Müller K, Preuster P, Bösmann A, Wasserscheid P. Highly efficient, low-temperature hydrogen release from perhydro-benzyltoluene using reactive distillation. Energy & Environmental Science. 2020;13:3119-28.
[49] Müller K, Thiele S, Wasserscheid P. Evaluations of Concepts for the Integration of Fuel Cells in Liquid Organic Hydrogen Carrier Systems. Energy & Fuels. 2019;33:10324-30.
[50] Haupt A, Müller K. Integration of a LOHC storage into a heat-controlled CHP system. Energy. 2017;118:1123-30.
[51] Keramiotis C, Stelzner B, Trimis D, Founti M. Porous burners for low emission combustion: An experimental investigation. Energy. 2012;45:213-9.
[52] Keramiotis C, Katoufa M, Vourliotakis G, Hatziapostolou A, Founti MA. Experimental investigation of a radiant porous burner performance with simulated natural gas, biogas and synthesis gas fuel blends. Fuel. 2015;158:835-42.
[53] Habib R, Yadollahi B, Saeed A, Doranehgard MH, Li LKB, Karimi N. Unsteady ultra-lean combustion of methane and biogas in a porous burner – An experimental study. Applied Thermal Engineering. 2021;182.
[54] Jaber A, Zigan L, Sakhrieh A, Leipertz A. Surface temperature measurements in a porous media burner using a new laser-induced phosphorescence intensity ratio technique. Measurement Science and Technology. 2013;24.
[55] Bollmann J, Schmidt N, Beck D, Preuster P, Zigan L, Wasserscheid P, et al. A path to a dynamic hydrogen storage system using a liquid organic hydrogen carrier (LOHC): Burner-based direct heating of the dehydrogenation unit. International Journal of Hydrogen Energy. 2022.
[56] Solymosi T, Auer F, Dürr S, Preuster P, Wasserscheid P. Catalytically activated stainless steel plates for the dehydrogenation of perhydro dibenzyltoluene. International Journal of Hydrogen Energy. 2021;46:34797-806.
[57] Auer F, Hupfer A, Bösmann A, Szesni N, Wasserscheidpeter P. Influence of the nanoparticle size on hydrogen release and side product formation in liquid organic hydrogen carrier systems with supported platinum catalysts. Catalysis Science & Technology. 2020;10:6669-78.
[58] Auer F. Katalysatorentwicklung für die Dehydrierung von Perhydro-Dibenzyltoluol [Dissertation]: FAU; 2020.
[59] Kolb S, Plankenbühler T, Hofmann K, Bergerson J, Karl J. Life cycle greenhouse gas emissions of renewable gas technologies: A comparative review. Renewable and Sustainable Energy Reviews. 2021;146:111147.
[60] Mrusek S, Preuster P, Müller K, Bösmann A, Wasserscheid P. Pressurized hydrogen from charged liquid organic hydrogen carrier systems by electrochemical hydrogen compression. International Journal of Hydrogen Energy. 2021;46:15624-34.
[61] Dürr S, Zilm S, Geißelbrecht M, Müller K, Preuster P, Bösmann A, et al. Experimental determination of the hydrogenation/dehydrogenation - Equilibrium of the LOHC system H0/H18-dibenzyltoluene. International Journal of Hydrogen Energy. 2021;46:32583-94.

[62] Geißelbrecht M. Prozessintensivierung für die Wasserstofffreisetzung aus flüssigen organischen Wasserstoffträgern [Doctoralthesis]: Friedrich-Alexander-Universität Erlangen-Nürnberg (FAU); 2021.